HHS Public Access

Author manuscript

Lab Anim (NY). Author manuscript; available in PMC 2021 April 27.

Published in final edited form as:

Lab Anim (NY). 2020 November ; 49(11): 320–334. doi:10.1038/s41684-020-00659-x.

Experimental murine arteriovenous fistula model to study restenosis after transluminal angioplasty

Chuanqi Cai[1,2], **Chenglei Zhao**[2,3], **Sreenivasulu Kilari**[2], **Amit Sharma**[2], **Avishek K. Singh**[2], **Michael L. Simeon**[2], **Avanish Misra**[2], **Yiqing Li**[1], **Sanjay Misra**[2,4,5]

[1]Department of Vascular Surgery, Union Hospital, Tongji Medical College, Huazhong University of Science and Technology, Wuhan, China.

[2]Vascular and Interventional Radiology Translational Laboratory, Department of Radiology, Mayo Clinic, Rochester, MN, USA.

[3]Department of Vascular Surgery, The Second Xiangya Hospital, Central South University, Changsha, China.

[4]Department of Biochemistry and Molecular Biology, Mayo Clinic, Rochester, MN, USA.

[5]Department of Radiology, Vascular and Interventional Radiology, Mayo Clinic, Rochester, MN, USA.

Abstract

Percutaneous transluminal angioplasty (PTA) is a very common interventional treatment for treating stenosis in arteriovenous fistula (AVF) used for hemodialysis vascular access. Restenosis occurs after PTA, resulting in vascular lumen loss and a decrease in blood flow. Experimental animal models have been developed to study the pathogenesis of stenosis, but there is no restenosis model after PTA of stenotic AVF in mice. Here, we describe the creation of a murine model of restenosis after angioplasty of a stenosis in an AVF. The murine restenosis model has several advantages, including the rapid development of restenotic lesions in the vessel after angioplasty and the potential to evaluate endovascular and perivascular therapeutics for treating restenosis. The protocol includes a detailed description of the partial nephrectomy procedure to induce chronic kidney disease, the AVF procedure for development of de novo stenosis and the

misra.sanjay@mayo.edu.

Author contributions

C.C. contributed to study design, animal surgeries, data collection, interpretation of data, and manuscript preparation. C.Z. contributed to study design, data analysis, and manuscript preparation. S.K. contributed to study design, interpretation of data, and manuscript review. A.S., A.K.S., M.L.S., A.M., and Y.L. contributed to interpretation of data, and manuscript review. S.M. contributed as a guarantor and to study design, interpretation of data and manuscript editing.

Competing interests

The authors declare no competing interests.

Additional information

Supplementary information is available for this paper at https://doi.org/10.1038/s41684–020-00659-x.

Reporting Summary

Further information on research design is available in the Nature Research Reporting Summary linked to this article.

Data availability

The data that support the findings of this study are available from the corresponding author upon request.

angioplasty treatment associated with progression of restenosis. We monitored the angioplasty-treated vessel for vascular patency and hemodynamic changes for a period of 28 d using ultrasound. Vessels were collected at different time points and processed for histological analysis and immunostaining. This angioplasty model, which can be performed with basic microvascular surgery skills, could be used to identify potential endovascular and perivascular therapies to reduce restenosis after angioplasty procedures.

Introduction

Although arteriovenous fistula (AVF) is the preferred hemodialysis vascular access for patients with end stage renal disease, the primary patency rate of AVF at 1 year is only 60%[1]. The low patency rate results from lumen vessel loss due to venous neointimal hyperplasia, which is caused by inflammation, hypoxia, shear stress and increased thrombogenicity[2]. Percutaneous transluminal angioplasty is used to treat stenosis in the arterial system as well as in AVF. Although percutaneous transluminal angioplasty is the first line of treatment for AVF stenosis, up to 50% of patients who undergo angioplasty present with restenosis within 6 months[3]. The exact mechanism of restenosis in AVF is unknown. Further understanding of the pathogenic mechanisms of restenosis may allow for the development of novel anti-restenotic treatments for patients with vascular stenosis.

To address this need, we developed a murine angioplasty restenosis model that allows the study of the interventional procedure in the early and late period[4]. This protocol was performed in 6- to 8-week-old female and male C57BL/6J mice. Angioplasty-treated vessels were evaluated longitudinally using ultrasound. In addition, we have used this model to assess the differences in gene expression and histomorphometric changes between male and female mice after angioplasty[5]. The model was also used to evaluate the potential of stem cell delivery to reduce restenosis after angioplasty[6]. This protocol may also be useful for the training of microvascular surgeons.

Comparison with other methods

Several animal species, including mice, rats, rabbits, sheep, dogs, pigs and primates, have been used to study the pathogenesis of AVF stenosis. Large animal models are useful for translational studies, but mechanistic evaluation can be difficult in these models, and their cost has reduced their use[7]. An article published in 2020 describes a restenosis model in male rat AVF with normal kidney function. The angioplasty procedure was performed in rats by using the Fogarty balloon catheter instead of a conventional angioplasty catheter[8]. The mouse model has many advantages, including the availability of transgenic knockout models to study mechanisms. To date, no mouse model of restenosis in AVF has been published.

Several different murine AVF models have been created, and they vary depending on the vessel used, type of anastomosis and configuration of the AVF. These models include the aortocaval puncture model[9], a model connecting the end of the ipsilateral carotid artery to the end of the ipsilateral jugular vein by using a plastic cuff[10], a model featuring an anastomosis between the end of the ipsilateral carotid artery and the end of the ipsilateral jugular vein[11], a model featuring an anastomosis between the end of the ipsilateral carotid

artery and the side of the ipsilateral jugular vein[12] and a model featuring an anastomosis between the side of the ipsilateral carotid artery and the end of the ipsilateral jugular vein[13]. All of these murine AVF models are valuable for our understanding of the mechanisms of neointimal hyperplasia but cannot be used for restenosis research, as the length and diameter of the vein, as well as available technology, are too limited to allow for the angioplasty procedure to be performed.

AVF models have been created in rats by using an anastomosis between the ipsilateral carotid artery and the jugular vein[14] and between the aorta and the inferior vena cava[15], as well as between the tail vessels[16] and femoral vessels[8]. The features of the stenosis in rats are similar to those in mice. Although AVFs have also been created in rabbits[17], dogs[18], sheep[19], pigs[20] and non-human primate animals[21], no model of angioplasty treatment of stenosis of an AVF has been described in these models.

The mouse AVF restenosis model after angioplasty described here might be an attractive option for researchers because of its reproducibility, reliability and relatively low cost. This model can also be used to study the mechanisms of restenosis by using knockout animals, small molecule inhibitors and restenotic drugs. Because of substantial differences between the mouse model and the human disease, successful therapies in murine models are rarely translated into clinical practice in humans[22,23]. However, current US Food and Drug Administration guidelines suggest that novel therapeutic agents should be tested in both small- and large-animal experiments[24]. Hemodialysis vascular access is created for patients with end stage renal disease. To mimic the clinical scenario of renal dysfunction, we created chronic kidney disease (CKD, Supplementary Fig. 1) and an AVF 28 d later. Therefore, this murine model of restenosis after angioplasty has clinically relevant features of renal dysfunction.

Applications and limitations

This protocol is not registered, and it is a useful tool for future studies aimed at elucidating the mechanisms driving restenosis induced by angioplasty of AVF and for therapeutic research. In addition, at the puncture site of the AVF, there is a normal vein segment that can be used to study puncture complications of interventional procedures. This murine angioplasty model has several advantages compared to larger-animal models, including that it comes with low cost and can be rapidly established. Furthermore, the present mouse model is described in C57BL/6J mice, which is the most popular strain in biomedical research. We have used this novel AVF-and-angioplasty model to describe the sex differences in AVFs and angioplasty-treated vessels and the delivery of adipose-derived mesenchymal stem cell therapy to prevent AVF restenosis[5,6,25]. Although the protocol described here was performed in C57BL/6J mice, it could be applied to other mouse strains and animal models, including rats, rabbits, dogs, pigs and primates.

Both AVF stenosis and arterial injury models present a similar vascular remodeling process, with cellular contributions from endothelial cells, vascular smooth muscle cells, fibroblasts, mesenchymal stem cells and inflammatory cells[2,26,27]. The angioplasty model might therefore also be used to further determine the source of cells contributing to restenosis. This model could also potentially be valuable for identifying therapeutic targets for arterial

restenosis and provides a new avenue to investigate in vivo the potential of chemical, stem cell, viral, nucleotide, stent implantation or protein-based therapy. Overall, this model can be used to study the mechanism and therapeutic outcomes linked to restenosis induced by angioplasty treatment.

Although this murine angioplasty procedure is performed in a stenotic vessel, the target vessel is an arterialized vein, which differs from a native artery structure. In the AVF segment of our murine model, the internal elastic lamina (IEL) is present, but the external elastic layer is absent. Moreover, angioplasty treatment ruptures the IEL, similar to the clinical procedure[4]. Arteriosclerosis is caused by increased cholesterol levels leading to lipid, endothelial and vascular smooth muscle cell dysfunction, which initiates inflammatory responses causing neointimal lesions[28]. Arteriosclerosis contributes to arterial restenosis after percutaneous coronary interventions[29] but is not common in AVF vessels. However, abnormal lipid metabolism is associated with AVF failure, which is similar to arterial stenosis and restenosis[30]. Arteriosclerosis is limited in the C57BL/6J AVF model, but this limitation can be addressed using *Apoe*$^{-/-}$ mice. The use of this protocol in *Apoe*$^{-/-}$ mice may enable the study of the relationship between hypercholesterolemia and angioplasty restenosis in mice. Finally, as we show in Supplementary Fig. 2, AVF vessels show substantial heterogeneity before angioplasty. The outflow vein illustrates this heterogeneity. When divided into different segments, there is more neointimal hyperplasia in the V3 segment, which is closer to the anastomosis compared to the V1 and V2 segments. The V1 segment is closer to the puncture site of the balloon catheter, and the V2 segment is where the majority of the injury after angioplasty occurs; V3 has more neointima than V2. V2 has been analyzed typically for histomorphometric readouts.

Development of the protocol

In this protocol, the main procedures include induction of CKD, creation of an AVF anastomosis and the subsequent angioplasty procedure of the stenotic AVF to establish a restenosis model. The smallest commercially available balloon catheter is a coronary size of 1.25-mm diameter with a 6.00-mm length. On the basis of published murine AVF models[10,13], the diameter of the vein was suitable for using this balloon catheter. However, the length of the vein was not adequate and needed to be longer. To address this, we used the end of the right external jugular vein (EJV) (REJV) and anastomosed it to the side of the left common carotid artery (LCCA), which provided an outflow vein length of 10 mm[4], thus making it possible to perform angioplasty. Histologically, stenosis develops in this model by 14 d after creation of the AVF, at which time angioplasty can be performed. To minimize bleeding, we dissected and clamped the inflow and outflow vessels. Angioplasty was performed by inserting the coronary balloon catheter through the distal segment of the outflow vein (V1) to the anastomosis. For sham controls, we dissected the outflow vein and inflow artery without angioplasty.

Experimental design

Age- and sex-matched mice should be randomly assigned to control and treatment groups. Mouse strains should be selected on the basis of the goal of the experiment. CKD was created by performing partial nephrectomy 4 weeks before placement of the AVF (Steps 1–

6). The major components of this angioplasty model include AVF creation (Steps 11–21) and angioplasty of the stenotic vessel (Steps 29–37).

Requirement for expertise—The angioplasty model requires technical skills, particularly mouse handling, microvascular surgical skills and the ability to perform angioplasty during the learning phase. To increase the reproducibility of the model, we suggest using at least one trained surgeon to perform the surgical procedures. AVF surgery can be completed by one person, while the angioplasty procedure should be completed by two persons, with one person responsible for stenotic vessel preparation while the other person performs balloon catheter inflation.

Surgical creation of AVF anastomosis—Although mice and humans have similar vascular terminology, there are five essential differences in the jugular vein between mice and humans. First, the REJV in mice is larger than the internal jugular vein and has several branches. Second, the REJV comprises two main branches, including the submental vein and the anterior facial vein. We selected the submental vein branch as the target vessel for AVF creation. Third, the LCCA is fully covered by the left sternocleidomastoid muscle, which needs to be removed during AVF creation. Fourth, the murine carotid sheath is thin, and the left vagus nerve is proximal to the LCCA, which should be dissected carefully to avoid injury. Finally, the REJV is anastomosed to the LCCA, which is anterior to the trachea, and it is essential to ensure that the REJV does not twist and become occluded during AVF creation and subsequent angioplasty.

Restenosis vessel follow-up—We used noninvasive Doppler ultrasound to monitor the vascular patency and hemodynamic changes in our model up to 28 d after angioplasty[4]. The jugular vein is superficial and in a fixed location. Technically, weekly Doppler ultrasound can be performed and is recommended to monitor changes in hemodynamics until the animal is sacrificed. In addition, the angioplasty-treated vessels can be analyzed at different time points to determine gene, protein and histological changes.

Administration of therapeutics—To study the effects of potential therapeutics on restenosis, mice should be randomly assigned to different groups, including vehicle control and treatment groups. Biologics or chemicals can be delivered by systemic, perivascular and endovascular routes with this protocol.

Mortality—Each mouse undergoes two or three surgeries, including CKD surgery, AVF creation and the angioplasty procedure. It is necessary to include sufficient mice in the experiment design to compensate for mortality after these procedures. In our experience, the main mortality of this model is from the AVF creation, especially for female mice because of a lower body weight and bleeding complications. The overall mortality for C57BL/6J mice is ~10% for AVF and angioplasty surgeries. Mortality might vary depending on the genetic background of the mice and the operator’s experience.

Materials

Biological materials

- 6- to 8-week-old male C57BL/6J mice (The Jackson Laboratory, cat. no. 000664) **! CAUTION** Approval from an institutional animal care and use committee must be obtained before performing any animal experiments. Approval from the Mayo Clinic Institutional Animal Care and Use Committee was obtained before starting this protocol ▲ **CRITICAL** In mice younger than 6 weeks old, mortality is increased due to mild bleeding during surgery because of the lower blood volume. In mice older than 8 weeks old, there is an excess of fat tissue surrounding the vessels, which makes vessel dissection and Doppler ultrasound more difficult to perform.

Reagents

- Sporicidin solution (Contec, Inc., cat. no. RE-1284F)
- General sterile solution (Sealed Air, Diversey Care, cat. no. 4277285)
- Povidone-iodine, 10% (wt/vol), paint (Carefusion, cat. no. 29906–008)
- Povidone-iodine, 7.5% (wt/vol), scrub (Carefusion, cat. no. 29904–016)
- Hair removal cream (Ardell Surgi-Cream, cat. no. 87–0717)
- Vet ointment (Paralube, National Drug Code (NDC) 17033–211-38; Dechra Veterinary)
- Electrocardiography coupling agent (Indus Instruments, cat. no. 600–0001-01-S)
- Sterile NaCl 0.9% (wt/vol), 1,000 ml, United States Pharmacopeia (USP) (Baxter Healthcare Corporation, cat. no. 2F7124)
- Sterile water for injection, 10 ml, USP (Hospira, cat. no. EN-3405)
- Sterile heparin sodium injection, 1,000 U/ml (Novaplus, cat. no. 402525D)
- Ketamine (100 mg/ml; NDC 0143–9509-01; West-Ward, cat. no. 1905034.1) **! CAUTION** Ketamin is a controlled substance. Follow institutional guidelines and practices.
- Xylazine (100 mg/ml; NDC 13985–704-10; VetOne, cat. no. V1510004) **! CAUTION** Xylazine is a controlled substance. Follow institutional guidelines and practices.
- Buprenorphine-SR (0.1 mg/ml; NDC 42023–179-05; Par Pharmaceutical, cat. no. 181099) **! CAUTION** Buprenorphine is a controlled substance. Follow institutional guidelines and practices.

Tissue collection

- RNA later (Qiagen, cat. no. 157025665)
- Formalin (Fisher Healthcare, cat. no. 305–510)

- Serum separator additive 400-μl tube (Microtainer; Becton Dickinson, cat. no. BD365967)

Equipment

- Small cotton-tipped applicators (Fisher Scientific, cat. no. 23–400-118)
- Pulsed Doppler device with heating pad (Indus Instruments, cat. nos. PDT-1704–0112 and DSD-1704–1224)
- Operative microscope (Leica Microsystems, cat. no. M125)
- Compak inflation pump (Merit Medical Systems, cat. no. IN4130)
- Coronary balloon catheter (Medtronic, Inc., cat. no. SPL12506X)
- Mouse-fixation band (3M, cat. no. 1527–1)
- Magnetic fixators with spring locks and retractor set (Kent Scientific Corporation, cat. nos. SURGI-5010–2 and SURGI-5016–2)
- Curved forceps (Fine Science Tools, cat. no. 11203–25)
- Straight forceps (Fine Science Tools, cat. no. 11251–30)
- Straight microsurgical clamps (S&T Microsurgical Instruments, cat. nos. 5111-B3V, 5308 B2V and 6370 B1V)
- Curved microsurgical clamps (Accurate Surgical & Scientific Instruments, cat. no. ASSI.R1A)
- Micro scissors (Fine Science Tools, cat. no. 15000–00)
- 1-ml 25-gauge tuberculin syringe (Covidien, cat. no. 8881501160)
- 23-gauge needle (Covidien, cat. no. 1188823100)
- 6–0 nonabsorbable braided silk suture (Fine Science Tools, cat. no. 18020–60)
- 8–0 sterile microsuture (Surgical Specialties, cat. no. AK-2508)
- 11–0 sterile nylon suture with threaded needle black polyamide monofilament non-absorbable (Aros Surgical Instruments, cat. no. T04A00N07–13)
- 6–0 vicryl absorbable sutures (Ethicon, cat. no. D5890)
- Heating pad for recovery (MATS; Leica, cat. no. 199807684)
- Sterile cage for recovery (Mayo Clinic Animal Facility)
- Surgical cautery (Cardinal Health, cat. no. 65410–010) **! CAUTION** Replace the cautery cap when not in use. For safe disposal, break off the tip with a hemostat and replace the cover cap. Failure to follow these instructions could result in fire.

Reagent setup

Ketamine/xylazine cocktail—Dilute ketamine and xylazine in sterile water. Use ketamine at 120 mg/kg body weight and xylazine at 10 mg/kg body weight for mouse intraperitoneal injection.

Heparin saline for heparinization—Dilute 5,000 U/ml heparin saline in sterile saline to use at 0.2 U/g for intravenous injection before clamping target vessels.

Heparin saline for vascular flushing—Dilute 5,000 U/ml heparin saline in sterile saline to use at 100 U/ml for endovascular flushing of the jugular vein and carotid artery. **! CAUTION** Heparin may cause hemorrhage in mice, and excessive saline injection may induce heart failure. The total volume of heparin saline injection is limited to 0.2 ml and the intravenous injection needs to be performed gently.

Equipment setup

Sterilize surgical instruments and sutures by submerging them in cold sterilant (Sporicidin solution) for 12 h. After sterilization, sterile saline is used to rinse the instruments. Wipe down all other equipment and surfaces with 5% (vol/vol) bleach. After shaving the murine neck area, the surgical area is sterilized by general sterile solution. The heating pad is set to 37 °C. The essential equipment used in AVF and angioplasty surgeries is presented in Fig. 1a–e. **! CAUTION** The person performing the animal surgery should follow aseptic operation principles to maintain a sterile field.

Procedure

Surgical preparation for mouse CKD surgery ● Timing ~5 min

1. Weigh the mouse and initiate anesthesia using ketamine/xylazine i.p. injection.

   ! CAUTION Procedures involving animals must be performed by qualified individuals according to institutional and national vertebrate animal welfare guidelines.

   ▲ **CRITICAL STEP** Confirm that the mouse is properly anesthetized by pinching a toe and verifying the absence of response.

2. Shave the hair of the mouse over the abdomen using an electric hair clipper and hair removal cream.

3. Place the animal in a supine position on the heating pad to maintain body temperature and continuously monitor heart and respiratory rates during surgery. Lubricate the eyes using vet ointment to prevent drying of the eyes during surgery. Disinfect the shaved area with alternating scrubs of 10% (wt/vol) and 7.5% (wt/vol) povidone-iodine using cotton swabs. Use isopropyl wipes between scrubs.

CKD procedure ● Timing ~10 min (surgical), 4 weeks (follow-up)

▲ **CRITICAL** See Supplementary Fig. 1a for visualization of the main steps of the CKD procedure

4. Create an abdominal midline incision (2.0 cm in length) and expose the left kidney (Supplementary Fig. 1b). Rotate the left kidney gently (Supplementary Fig. 1c) to dissect the bifurcation of the left main renal artery (Supplementary Fig. 1d). Ligate the upper branch of the left renal artery (Supplementary Fig. 1d, white arrow) with 6–0 silk suture. Expose the right kidney and ligate the right ureter (Supplementary Fig. 1e), renal artery and vein (Supplementary Fig. 1f) with 6–0 silk suture. Cut the right ureter and vessels and remove the whole right kidney (Supplementary Fig. 1g).

   ▲ **CRITICAL STEP** Be gentle during the dissection of the left renal artery to avoid rupture of the renal vein. The right renal artery and vein should be double-ligated to avoid potentially fatal bleeding.

   ? TROUBLESHOOTING

5. Confirm successful CKD surgery by observing immediate ischemia to the upper pole of the left kidney (Supplementary Fig. 1h). In addition, 4 weeks later, necrosis and atrophy of the upper pole of the left kidney can be observed (Supplementary Fig. 1i).

   ? TROUBLESHOOTING

6. Close the abdominal muscle and skin with a running 6–0 vicryl absorbable suture.

7. Turn the mouse prone after closing the incision. Inject the animal with 0.05–0.10 mg/kg of buprenorphine-SR (s.c.) analgesic immediately.

8. Allow the animal to recover from anesthesia on a heating pad to maintain body temperature. Monitor the mouse until it exhibits normal breathing and behavior.

9. Transfer the animal to a clean cage and housing with ad libitum access to water and food.

10. Monitor the animal daily for the first week after surgery and then weekly until the AVF surgery.

    ▲**CRITICAL STEP** Additional analgesics are necessary if the animal exhibits signs of pain or distress beyond 72 h.

    ▲ **CRITICAL STEP** To confirm the presence of renal dysfunction after CKD surgery, blood should be collected for blood urea nitrogen and creatinine assays before CKD surgery (at day (D) −42) and before AVF surgery (at D−14; Supplementary Fig. 1, j and k).

Surgical preparation for mouse AVF surgery ● Timing ~5 min

11. Weigh the mouse and initiate anesthesia using a ketamine/xylazine i.p. injection.

▲ **CRITICAL STEP** Confirm that the mouse is properly anesthetized by pinching a toe and verifying the absence of response.

12. Shave the hair in the front neck area using an electric hair clipper and hair removal cream.

13. Place the animal in a supine position on the heating pad to maintain body temperature and continuously monitor heart and respiratory rates during the surgery. Lubricate the eyes using vet ointment to prevent drying of the eyes during surgery. Disinfect the shaved area with two alternating scrubs of 10% (wt/vol) and 7.5% (wt/vol) povidone-iodine using cotton swabs, swabbing the area with isopropyl wipe between scrubs.

▲ **CRITICAL STEP** It is important to perform continuous monitoring of vital signs while the animal is under anesthesia. An increasing heart rate indicates that the anesthesia is subsiding, and an extra dose of anesthesia will be necessary to complete the surgery. Intraoperative Doppler ultrasound of the AVFs needs to be performed within a similar range of heart rate for each mouse.

AVF anastomosis procedure ● Timing ~40 min

▲ **CRITICAL** See Fig. 1f and Supplementary Video 1 for visual instructions on the AVF procedure.

14. Make a curved incision (2.5 cm in length) parallel to the right side of the trachea (Fig. 1g). Dissect the subcutaneous tissue, fat tissue and muscle layer by layer. Ligate the proximal end of the cephalic vein and the anterior facial vein using an 8–0 nylon suture and the distal end with a 6–0 silk suture. The rest of the branches of the REJV are cauterized using an electronic cutter. The final length of the REJV should be ≥10 mm (Fig. 1h).

▲ **CRITICAL STEP** Be gentle during the dissection of the REJV, to avoid rupture of the vein.

? TROUBLESHOOTING

15. Isolate and remove the left sternocleidomastoid muscle when preparing the LCCA. The whole LCCA (3 mm in length) is dissected while keeping the left vagus nerve intact.

▲ **CRITICAL STEP** The left vagus nerve is critical for survival.

? TROUBLESHOOTING

16. Ligate the distal end and cut the proximal end of the REJV. Inject 0.2 U/g of heparin through the puncture created in the REJV. Two minutes later, clamp the REJV and the LCCA, respectively (Fig. 1i).

▲ **CRITICAL STEP** Heparinized saline needs to be injected before vascular clamping to avoid acute postoperative thrombosis.

17. Flush the vessel lumen of the REJV and the LCCA to remove all potential thrombi. Before creating the anastomosis, confirm that the REJV is not kinked or

twisted. Use micro scissors to create a parallel incision on the front side of the LCCA (1.0-mm length). Anastomose the end of the REJV to the side of the LCCA using an 11–0 suture (Fig. 1j). Briefly, fix the REJV to the LCCA with an interrupted suture at the six o'clock position, and then use the continuous suture technique starting at the twelve o'clock position of the back side to the front side.

▲ **CRITICAL STEP** Confirm that the vessel is not kinked or twisted, and full flushing of the lumen is necessary. To avoid aneurysmal dilation of the anastomosis, we used the continuous suture technique and placed eight stitches.

? TROUBLESHOOTING

18. Unclamp the REJV first, followed by the distal LCCA. Check that there is no obvious bleeding from the AVF. The red color from the arterial flow from the LCCA into the REJV will be seen. Unclamp the proximal LCCA and handle mild bleeding by gentle compression using a cotton tip.

▲ **CRITICAL STEP** The sequence for unclamping the vein and artery is important.

? TROUBLESHOOTING

19. Evaluate the AVF patency and function immediately by performing Doppler ultrasound examination of the inflow artery, outflow vein and contralateral artery.

▲ **CRITICAL STEP** Doppler ultrasound evaluation is useful for the assessment of the AVF. The surface of the vessel should appear wet and glistening.

20. The anastomosis angle should be 90°. Remove any residual sutures from the surgical site and irrigate the AVF with sterile saline.

▲ **CRITICAL STEP** This is the last chance to ensure that there is no twisting of the AVF. The anastomosis angle must be similar for all animals for reproducibility and to reduce bias.

21. Close the subcutaneous muscle and skin with a running 6–0 vicryl absorbable suture.

22. Turn the mouse prone after closing the incision. Inject the animal with 0.05–0.10 mg/kg of buprenorphine-SR (s.c.) analgesic immediately.

23. Allow the animal to recover from anesthesia on a heating pad to maintain body temperature. Monitor the mouse until it exhibits normal breathing and behavior.

24. Transfer the animal to a clean cage and housing with ad libitum access to water and food.

25. Monitor the animal twice a day for the first week after surgery and then once daily until the angioplasty surgery 14 d later.

▲ **CRITICAL STEP** Additional analgesics are necessary if the animal exhibits signs of pain or distress beyond 72 h.

Surgical preparation for mouse angioplasty surgery ● Timing ~5 min

26. Weigh the mouse and complete anesthesia using a ketamine/xylazine i.p. injection.

▲ **CRITICAL STEP** Confirm that the mouse is properly anesthetized and shows no response after toe-pinching.

27. Shave the hair of the mouse in the front of the neck using an electric hair clipper and hair removal cream.

28. Place the animal supine on the heating pad to maintain body temperature and continuously monitor heart and respiratory rates during surgery. Lubricate the eyes to prevent drying of the eyes during the operation. Disinfect the shaved area with two alternating scrubs of 10% (wt/vol) and 7.5% (wt/vol) povidone-iodine using cotton swabs, swabbing the area with isopropyl wipe between scrubs.

▲ **CRITICAL STEP** Continuous monitoring is required while the mouse is under anesthesia.

Angioplasty surgical procedure ● Timing ~25 min

▲ **CRITICAL** See Supplementary video 2 for visual instructions on the angioplasty procedure.

29. Make one horizontal incision (2.0 cm in length) along the scar from the AVF surgery. Dissect the subcutaneous tissues and fat tissue. Retract salivary glands to facilitate exposure of the REJV. Dissect the entire REJV to identify the location for the puncture of the angioplasty catheter (Fig. 1k).

30. Dissect the inflow artery and outflow vein without inducing any injury to the left vagus nerve.

▲ **CRITICAL STEP** Dissection should be gentle, to avoid damage to the blood vessels and the left vagus nerve.

? TROUBLESHOOTING

31. Clamp the distal LCCA and proximal LCCA, sequentially. Inject 0.2 U/g of heparin through the puncture created in the REJV. Two minutes later, clamp the REJV.

▲ **CRITICAL STEP** Clamping the vessels in the correct order is important. Heparinized saline injection is necessary before the angioplasty procedure to replicate clinical practice.

32. Flush the lumen of the AVF with heparinized saline through the puncture. Before performing the angioplasty procedure, measure the length of the REJV to determine if it is suitable for angioplasty (Fig. 1l).

▲ **CRITICAL STEP** Flush the REJV with heparinized saline before the angioplasty procedure to remove potential thrombi.

▲ **CRITICAL STEP** The length of the REJV should be greater than the length of the balloon.

33. Insert a deflated balloon catheter through the puncture point to the anastomosis area covering all of the stenotic lesion area. Use a connected pump to slowly inflate the balloon catheter from 0 to 14 atm. Hold at 14 atm for 30 s and then deflate and remove the balloon. The enlarged targeted vessel is observable with a microscope vision lens (Fig. 1m).

▲ **CRITICAL STEP** The angioplasty procedure should be performed under a microscope vision lens, and the inflation pressure should not exceed 14 atm.

? TROUBLESHOOTING

34. After successful angioplasty, flush the vessel with heparinized saline. Suture the puncture using a continuous 11–0 suture with four stitches. Unclamp the REJV, distal LCCA and proximal LCCA in this order (Fig. 1n).

▲ **CRITICAL STEP** Flush the vessel lumen to eliminate any thrombi. Unclamping of vessels should be done in the correct order after the puncture is closed. Continuous suture technique with four stitches is applied for the closure of the angioplasty puncture site, and too many stitches can cause a stenosis to form.

? TROUBLESHOOTING

35. (Optional) Endovascular administration of therapeutics should be done before closing the puncture. Perivascular delivery should be done after closing the puncture.

36. After restoring blood flow, evaluate the patency and function of the angioplasty-treated vessel using Doppler ultrasound, including the inflow artery, outflow vein and contralateral artery.

▲ **CRITICAL STEP** Doppler ultrasound is useful to evaluate angioplasty treatment. The surface of the vessels should be wet and glistening.

37. Close the subcutaneous layer and skin with a running 6–0 vicryl absorbable suture.

38. Turn the mouse prone after closing the incision. Administer one dose of buprenorphine-SR (0.05–0.10 mg/kg s.c.) immediately.

39. Allow the animal to recover from anesthesia on a heating pad to maintain body temperature. Monitor the mouse until it exhibits normal breathing and behavior.

40. Transfer the animal to a clean cage and house individually with ad libitum access to water and food.

41. Monitor the mouse two times per day for the first week after the angioplasty procedure and then once daily until sacrifice.

▲ **CRITICAL STEP** Additional analgesics are necessary if the animal exhibits signs of pain or distress beyond 72 h.

Post-operative assays ● Timing variable

42. At the desired experimental endpoint, euthanize the animals according to your institutionally approved method. We exsanguinated the animals by removing blood from the inferior vena cava after the noninvasive Doppler ultrasound detection.

▲ **CRITICAL STEP** During euthanasia, flush the REJV with saline to avoid any thrombi formation.

43. Collect the target vessel for histological analysis. Flush 5 ml of formalin through the ascending aorta before removing the target vessel. Incubate the vessel at 4 °C overnight in formalin to fix the tissue. For qRT-PCR analysis, the vessel should be flushed with saline and stored in RNA later reagent at −80 °C.

44. Each angioplasty-treated vessel should be embedded in paraffin lengthwise. Alternatively, tissue can be fixed in optimal cutting temperature (OCT) compound using the standard cryo-embedding protocol.

▲ **CRITICAL STEP** Because of the heterogeneity of this AVF model, we suggest using the V2 segment for the histological analysis, as shown in Supplementary Fig 2.

■ **PAUSE POINT** To avoid potential false-negative immunostaining, unstained paraffin slices should be stored for <12 weeks[31].

45. Section the paraffin blocks. Typically, an average of 40–60 consecutive 4-μm sections will be obtained per vessel per animal for analysis. Perform immunohistochemistry analysis of the slices.

Troubleshooting

Troubleshooting advice for CKD surgery, AVF creation and the angioplasty procedure can be found in Table 1.

Timing

The times listed below refer to the handling of one mouse.

Steps 1–6, partial nephrectomy surgery: ~15 min

Steps 7–10, recovery and follow-up: 28 d

Steps 11–13, anesthesia and mice preparation for AVF surgery: ~5 min

Steps 14–16, exposure of the REJV: ~15 min

Steps 17 and 18, AVF anastomosis procedure: ~20 min

Steps 19–21, Doppler ultrasound detection and incision closure: ~5 min

Steps 22–25, recovery: 4 h, follow-up: 14 d

Steps 26–28, anesthesia and mice preparation for angioplasty surgery: ~5 min

Steps 29–32, exposure of the inflow artery and the outflow arterialized vein: ~15 min

Steps 33–35, angioplasty procedure (with or without delivery of therapeutics): ~5 min

Steps 36 and 37, Doppler ultrasound detection and incision closure: ~5 min

Steps 38–41, recovery: 4 h, follow-up: up to 28 d

Steps 42 and 43, Doppler ultrasound detection and tissue collection: ~30 min

Steps 44 and 45, specimen disposal: timing varies depending on the tissue-processing protocols

Anticipated results

Below, we present the anticipated results for the analysis of 8-week-old male C57BL/6J mice. We randomly assigned mice to the angioplasty-treated group (day 0 after sham/angioplasty procedure (D0-post): $n = 6$; D14: $n = 6$; D28: $n = 6$) or the sham group (D0-post: $n = 6$; D14: $n = 6$; D28: $n = 6$). Each mouse underwent a partial nephrectomy for CKD, an AVF creation for stenosis and an angioplasty procedure for restenosis, following the timeline described in Fig. 2a. There was no endovascular or perivascular intervention in the angioplasty-treated vessels. Vessels were collected and processed. Slides were processed for H&E, Verhoeff–Van Gieson (VVG) and immunostaining; images were digitized and analyzed in a blinded fashion (time points and sham/angioplasty groups were not known). Sex is a variable that can affect the outcomes in angioplasty procedures, as we reported previously[5]. Age is another important factor linked to vascular remodeling[32]. The histomorphometric results could also vary between different genetically engineered mice. All these factors, therefore, should be considered in the experimental design.

Time course of stenosis and restenosis in the murine angioplasty model

CKD surgery, AVF creation and the angioplasty procedure were performed sequentially as shown in Fig. 2a. After AVF creation (D−14), the outflow vein became arterialized. In the sham group for which no angioplasty was performed, we observed a decreased vascular lumen area and increased neointimal area/media area (N/M ratio) at D14 compared to D0 (Fig. 2b, upper panel). In addition, in sham vessels, at D28 the vessel lumen area decreased compared to D0 and D14, which indicates continuous vessel lumen loss. By contrast, at D0-post, the REJV had less neointimal area than in the sham group (Fig. 2b, lower panel). We performed VVG staining on sections from the contralateral jugular vein, sham vessel and angioplasty-treated vessel at D14 (Fig. 2c). An intact and continuous IEL was seen in the sham vessel, but the IEL was broken after angioplasty.

We performed Doppler ultrasound, which revealed no significant difference between sham vessels and angioplasty-treated vessels at D0 after sham/angioplasty. After angioplasty, there was a significant increase in the peak velocity of the angioplasty vessels compared to those in sham controls at D14 (average increase: 72%, $P = 0.0004$; Fig. 2d).

The intraoperative in vivo vascular diameter was measured (Fig. 2e). At D0-post, both sham- and angioplasty-treated vessels showed a significant increase in the vascular diameter compared to D−14 (sham, average increase: 58%, $P < 0.0001$; angioplasty, average increase: 58%, $P < 0.0001$), indicating outward remodeling after AVF creation (Fig. 2e). In the sham group, the vascular diameter decreased from D14 to D28, whereas in the angioplasty group, the reduction in vascular diameter was less important (Fig. 2e). At D14, there was a significant increase in the vascular diameter of the angioplasty-treated vessels compared to the sham vessels, which was abolished at D28 (Fig. 2e).

At D0, angioplasty-treated vessels showed a significantly smaller vessel lumen area compared to sham vessels (average decrease: 52%, $P = 0.0080$; Fig. 2f), and this may be linked to elastic recoil after angioplasty[33]. At D14, angioplasty-treated vessels showed significantly larger vessel lumen area compared to sham vessels (average increase: 68%, $P = 0.0096$; Fig. 2f). However, there was no significant difference in the vessel lumen area between the two groups at D28 (Fig. 2f). We have previously demonstrated that the angioplasty procedure leads to a decrease in neointimal hyperplasia in the early period after interventional treatment[4].

In the sham mice, there was a significant increase in the N/M ratio at D14 compared to D0 ($P = 0.0544$; Fig. 2g) and at D28 compared to D0 ($P = 0.0090$; Fig. 2g). The angioplasty-treated vessels also showed a similar increase in the N/M ratio at D14 compared to D0 ($P = 0.0227$; Fig. 2g) and D28 compared to D0 ($P < 0.0001$; Fig. 2g). However, angioplasty-treated vessels had a significant decrease in N/M ratio at D0 (average decrease: 56%, $P = 0.0238$; Fig. 2g), D14 (average decrease: 63%, $P < 0.0001$; Fig. 2g) and D28 (average decrease: 30%, $P = 0.0314$; Fig. 2g) compared to sham vessels.

Altogether, these morphometric data suggest that the angioplasty procedure induces a break in the IEL and a significant increase in the peak velocity, vascular diameter and vessel lumen area and a decrease in the N/M ratio at D14. However, at D28 there was no difference in the average peak velocity, vascular diameter, vessel lumen area and N/M ratio between angioplasty-treated vessels and sham vessels. D14 could be the suitable time point for the study of early restenosis linked to angioplasty treatment, and D28 could be suitable to study restenotic and neointimal hyperplasia.

Immunostaining for endothelial cells (CD31), vascular smooth muscle cells (alpha-smooth muscle actin (α-SMA)) and cellular proliferation (Ki-67) at different time points

Endothelial injury can result in restenosis leading to AVF failure[2,34]. We performed CD31 immunostaining to assess the endothelium in sham- and angioplasty-treated vessels using the EnVision protocol after heat-induced antigen retrieval[4]. As we reported previously[4], although the angioplasty procedure denudated the endothelium at D0 (Fig. 3a, left panel), re-endothelialization could be seen at D14 (Fig. 3a, middle panel). In the sham vessels, the

endothelium was not intact and was accompanied with neointimal hyperplasia (Fig. 3a). However, at D28, both sham- and angioplasty-treated vessels presented with a discontinuous endothelial layer (Fig. 3a, right panel). Semi-quantitative analysis showed that there was a significant decrease in the CD31 index of angioplasty-treated vessels compared to sham vessels (average decrease: 95%, $P < 0.0001$; Fig. 3b) at D0-post, as well as a significant increase (average increase: 85%, $P < 0.0001$; Fig. 3b) at D14, with no difference at D28 ($P > 0.9999$; Fig. 3b).

Vascular smooth muscle cell accumulation and increased cellular proliferation are common pathological changes in restenotic lesions and AVF neointimal hyperplasia[2,35]. We performed α-SMA (Fig. 4) and Ki-67 (Fig. 5) staining to determine the smooth muscle cell deposition and cellular proliferation in sham- and angioplasty-treated vessels. First, at D0-post, there were less $\alpha\text{-SMA}^+$ cells in angioplasty-treated vessels (Fig. 4a, left panel). In addition, at D0 there was a lower Ki-67 index of angioplasty-treated vessels than of sham controls (average increase: 24%, $P = 0.0076$; Fig. 5a,b). As expected, at D14 fewer α-SMA (Fig. 4a, middle panel) and Ki-67 (Fig. 5a, middle panel) positive cells were observed in the neointimal area of angioplasty-treated vessels compared to sham controls. Interestingly, at D28 both sham- and angioplasty-treated vessels showed decreased α-SMA staining compared to D14 vessels (Fig. 4a, right panel). This observation is consistent with the decreased Ki-67 staining at D28 (Fig. 5a, right panel). Semiquantitative analysis at D14 showed a significant reduction in the α-SMA index (average decrease: 51%, $P = 0.0007$; Fig. 4b) and Ki-67 index (average decrease: 44%, $P = 0.0123$; Fig. 5b) of angioplasty-treated vessels compared to sham controls. There were no significant differences in the α-SMA ($P = 0.6617$; Fig. 4b) and Ki-67 ($P > 0.9999$; Fig. 5b) indexes at D28 between sham- and angioplasty-treated vessels.

Altogether, these data indicate that re-endothelialization occurs after the angioplasty procedure, but subsequent disruption of the endothelial layer may be associated with restenosis. Positive α-SMA and Ki-67 cells were mainly observed at D14 and not D28 in the outflow vessels. This result is consistent with other published data showing that smooth muscle cell accumulation and proliferation occur in the early period[35].

Perivascular and endovascular delivery for anti-restenosis after the angioplasty procedure

Several methods can be used for anti-restenotic treatment, including systemic, perivascular and endo vascular delivery of biologics. Perivascular and endovascular delivery are associated with fewer adverse effects to other organs and with higher local concentration of therapy to the angioplasty-treated vessel. After the angioplasty procedure (Fig. 6a), before restoring blood flow, endovascular therapy can be delivered as shown in Fig. 6b. Adventitial cells are linked to restenosis after angioplasty treatment[36]. In Fig. 6c we show successful delivery of drug-loaded biocompatible poly lactic-*co*-glycolic acid nanoparticles in hydrogel to the perivascular tissue after angioplasty (unpublished image). In addition, we have delivered adipose-derived mesenchymal stem cells to the adventitia of angioplasty-treated vessels to alleviate the restenosis[6]. These different methods for drug delivery could be beneficial in the assessment of novel therapies for restenosis.

In summary, this protocol provides a detailed technical approach to reproducibly create restenosis after an angioplasty procedure in a murine model. The use of this method has demonstrated the feasibility of exploring novel treatments to target restenosis. We propose that this protocol can be used to test novel therapeutic treatment for vascular stenosis and restenosis.

Supplementary Material

Refer to Web version on PubMed Central for supplementary material.

Acknowledgements

The authors acknowledge the assistance of Lucy Bahn, PhD for editing the manuscript. This research was supported by NIH grants to S.M. (HL098967 and DK107870).

References

1. Al-Jaishi AA et al. Patency rates of the arteriovenous fistula for hemodialysis: a systematic review and meta-analysis. Am. J. Kidney Dis 63, 464–478 (2014). [PubMed: 24183112]
2. Brahmbhatt A, Remuzzi A, Franzoni M. & Misra S. The molecular mechanisms of hemodialysis vascular access failure. Kidney Int. 89, 303–316 (2016). [PubMed: 26806833]
3. Bountouris I, Kritikou G, Degermetzoglou N. & Avgerinos KI A review of percutaneous transluminal angioplasty in hemodialysis fistula. Int. J. Vasc. Med 2018, 1420136 (2018).
4. Cai C. et al. Evaluation of venous stenosis angioplasty in a murine arteriovenous fistula model. J. Vasc. Interv. Radiol 30, 1512–1521.e3 (2019).
5. Cai C. et al. Effect of sex differences in treatment response to angioplasty in a murine arteriovenous fistula model. Am. J. Physiol. Renal Physiol 318, F565–F575 (2020). [PubMed: 31813252]
6. Cai C. et al. Therapeutic effect of adipose derived mesenchymal stem cell transplantation in reducing restenosis in a murine angioplasty model. J. Am. Soc. Nephrol 31, 1781–1795 (2020). [PubMed: 32587073]
7. Geary RL et al. Time course of cellular proliferation, intimal hyperplasia, and remodeling following angioplasty in monkeys with established atherosclerosis. A nonhuman primate model of restenosis. Arterioscler. Thromb. Vasc. Biol 16, 34–43 (1996). [PubMed: 8548423]
8. Somarathna M, Isayeva-Waldrop T, Al-Balas A, Guo L. & Lee T. A novel model of balloon angioplasty injury in rat arteriovenous fistula. J. Vasc. Res 57, 223–235 (2020). [PubMed: 32396897]
9. Yamamoto K, Li X, Shu C, Miyata T. & Dardik A. Technical aspects of the mouse aortocaval fistula. J. Vis. Exp 77, e50449–e50449 (2013).
10. Yang B, Shergill U, Fu AA, Knudsen B. & Misra S. The mouse arteriovenous fistula model. J. Vasc. Interv. Radiol 20, 946–950 (2009). [PubMed: 19555889]
11. Liang A, Wang Y, Han G, Truong L. & Cheng J. Chronic kidney disease accelerates endothelial barrier dysfunction in a mouse model of an arteriovenous fistula. Am. J. Physiol. Renal Physiol 304, F1413–F1420 (2013). [PubMed: 23576636]
12. Castier Y. et al. Characterization of neointima lesions associated with arteriovenous fistulas in a mouse model. Kidney Int. 70, 315–320 (2006). [PubMed: 16760906]
13. Kang L. et al. A new model of an arteriovenous fistula in chronic kidney disease in the mouse: beneficial effects of upregulated heme oxygenase-1. Am. J. Physiol. Renal Physiol 310, F466–F476 (2016). [PubMed: 26672617]
14. Croatt AJ et al. Characterization of a model of an arteriovenous fistula in the rat: the effect of L-NAME. Am. J. Pathol 176, 2530–2541 (2010). [PubMed: 20363917]
15. Manning E. et al. A new arteriovenous fistula model to study the development of neointimal hyperplasia. J. Vasc. Res 49, 123–131 (2012). [PubMed: 22249138]

16. Lin T, Horsfield C. & Robson MG Arteriovenous fistula in the rat tail: a new model of hemodialysis access dysfunction. Kidney Int. 74, 528–531 (2008). [PubMed: 18509320]
17. Li Z. et al. Hyperbaric oxygen inhibits venous neointimal hyperplasia following arteriovenous fistulization. Int. J. Mol. Med 39, 1299–1306 (2017). [PubMed: 28393184]
18. Masaki T. et al. Inhibition of neointimal hyperplasia in vascular grafts by sustained perivascular delivery of paclitaxel. Kidney Int. 66, 2061–2069 (2004). [PubMed: 15496180]
19. Florescu MC et al. Sheep model of hemodialysis arteriovenous fistula using superficial veins. Semin. Dial 28, 687–691 (2015). [PubMed: 26189959]
20. Loveland-Jones CE et al. A new model of arteriovenous fistula to study hemodialysis access complications. J. Vasc. Access 15, 351–357 (2014). [PubMed: 24811594]
21. Kraiss LW et al. Acute reductions in blood flow and shear stress induce platelet-derived growth factor-A expression in baboon prosthetic grafts. Circ. Res 79, 45–53 (1996). [PubMed: 8925568]
22. Lafont A. & Faxon D. Why do animal models of post-angioplasty restenosis sometimes poorly predict the outcome of clinical trials? Cardiovasc. Res 39, 50–59 (1998). [PubMed: 9764189]
23. Le Bras A. A resource for selecting animal models of heart disease. Lab Anim. 48, 332 (2019).
24. Hartung T. Rebooting the generally recognized as safe (GRAS) approach for food additive safety in the US. ALTEX 35, 3–25 (2018). [PubMed: 29374436]
25. Cai C. et al. Differences in transforming growth factor-β1/BMP7 signaling and venous fibrosis contribute to female sex differences in arteriovenous fistulas. J. Am. Heart Assoc 9, e017420 (2020).
26. Gibbons GH & Dzau VJ The emerging concept of vascular remodeling. N. Engl. J. Med 330, 1431–1438 (1994). [PubMed: 8159199]
27. Abedin M, Tintut Y. & Demer LL Mesenchymal stem cells and the artery wall. Circ. Res 95, 671–676 (2004). [PubMed: 15459088]
28. Ross R. Atherosclerosis—an inflammatory disease. N. Engl. J. Med 340, 115–126 (1999). [PubMed: 9887164]
29. Jukema JW, Verschuren JJW, Ahmed TAN & Quax PHA Restenosis after PCI. Part 1: pathophysiology and risk factors. Nat. Rev. Cardiol 9, 53–62 (2012).
30. De Marchi S. et al. Risk factors for vascular disease and arteriovenous fistula dysfunction in hemodialysis patients. J. Am. Soc. Nephrol 7, 1169–1177 (1996). [PubMed: 8866409]
31. Bertheau P. et al. Variability of immunohistochemical reactivity on stored paraffin slides. J. Clin. Pathol 51, 370–374 (1998). [PubMed: 9708203]
32. Ungvari Z, Tarantini S, Donato AJ, Galvan V. & Csiszar A. Mechanisms of vascular aging. Circ. Res 123, 849–867 (2018). [PubMed: 30355080]
33. Caixeta AM et al. [Analysis of elastic retraction in the 1st 15 minutes after coronary balloon angioplasty]. Arq. Bras. Cardiol 66, 5–9 (1996). [PubMed: 8731316]
34. Meurice T. et al. Role of endothelial cells in restenosis after coronary angioplasty. Fundam. Clin. Pharmacol 10, 234–242 (1996). [PubMed: 8836697]
35. Hanke H, Strohschneider T, Oberhoff M, Betz E. & Karsch KR Time course of smooth muscle cell proliferation in the intima and media of arteries following experimental angioplasty. Circ. Res 67, 651–659 (1990). [PubMed: 1697794]
36. Staab ME et al. Arterial remodeling after experimental percutaneous injury is highly dependent on adventitial injury and histopathology. Int. J. Cardiol 58, 31–40 (1997). [PubMed: 9021425]

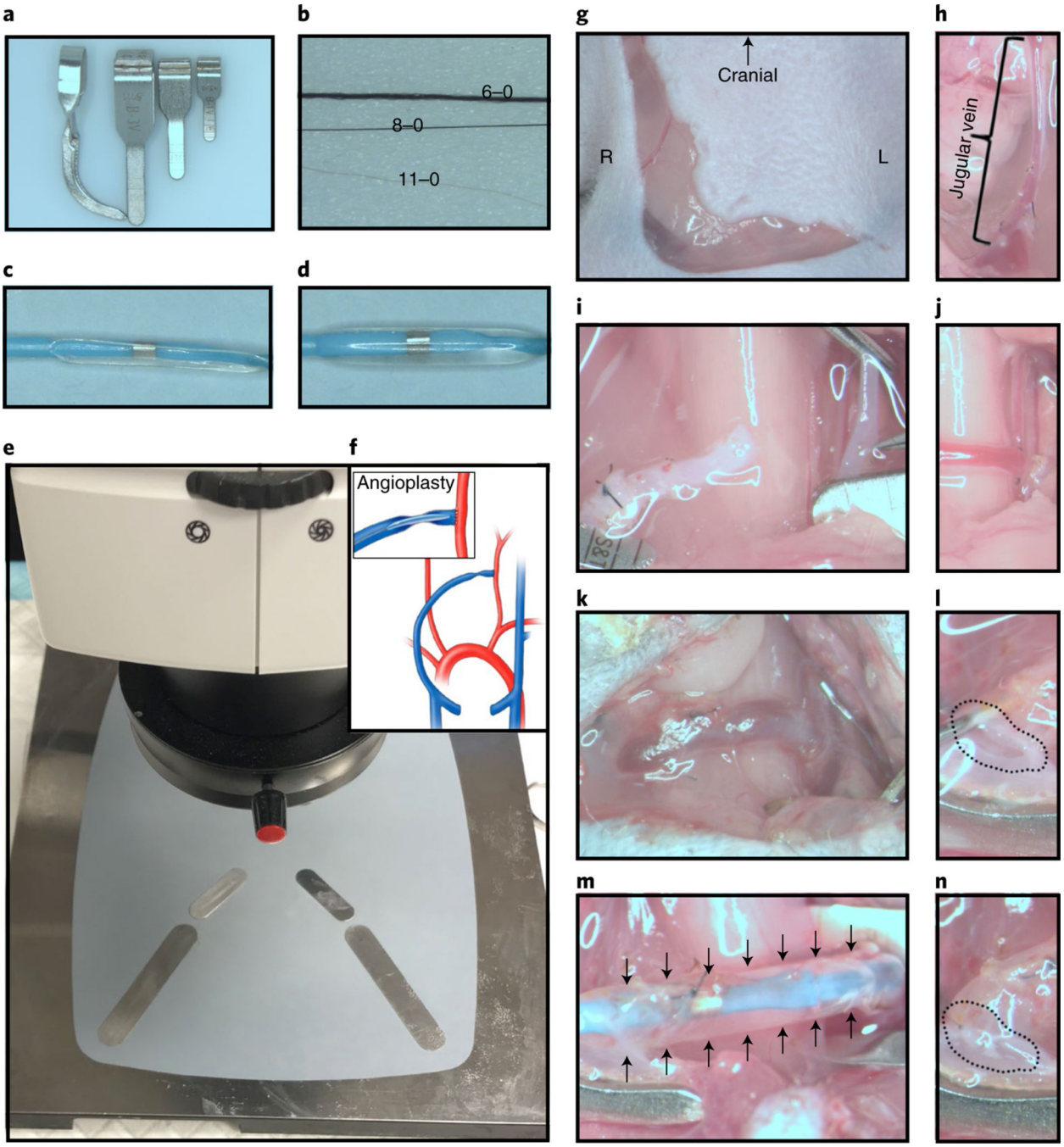

Fig. 1 |. Materials required and technical procedures for CKD, AVF and angioplasty procedures.
a, Different sizes of microvascular clamps for different vessel diameters: the smallest one is only for clamping the vein, and the others are used for arterial and EJV clamping. **b**, Different sutures for ligating and creating the vascular anastomosis: the 6–0 silk suture is for ligation of the distal end of the EJV, 8–0 is for ligation of the proximal end of the EJV and the 11–0 suture is for AVF anastomosis and closure of the puncture used for inserting the angioplasty catheter. **c**, Deflated 1.25 mm × 6 mm balloon catheter. **d**, Inflated balloon catheter at 14 atm pressure. **e**, Experimental setup before anesthetizing the mouse. **f**,

Schematic of AVF creation and angioplasty procedures. **g**, Curved incision in the right neck paralleling the trachea. **h**, The right EJV should be dissected ≥10 mm in length. **i**, The REJV and LCCA are flushed with heparinized saline before creating the AVF anastomosis. **j**, After the AVF anastomosis has been created, red pulsatile arterial blood flow is observed in the outflow vein. **k**, Two weeks after creating the AVF anastomosis, the arterialized EJV has an enlarged diameter. **l**, After clamping the inflow and outflow vessels, the vessels are flushed with heparinized saline through the puncture site. **m**, The angioplasty is performed at 14 atm for 30 s. **n**, The angioplasty puncture site is closed using an 11–0 suture. R, Right side; L, left side. Black arrows indicate the inflated balloon catheter, and the dashed circles indicate the puncture site. Animal procedures in this work were approved by the Mayo Clinic Institutional Animal Care and Use Committee.

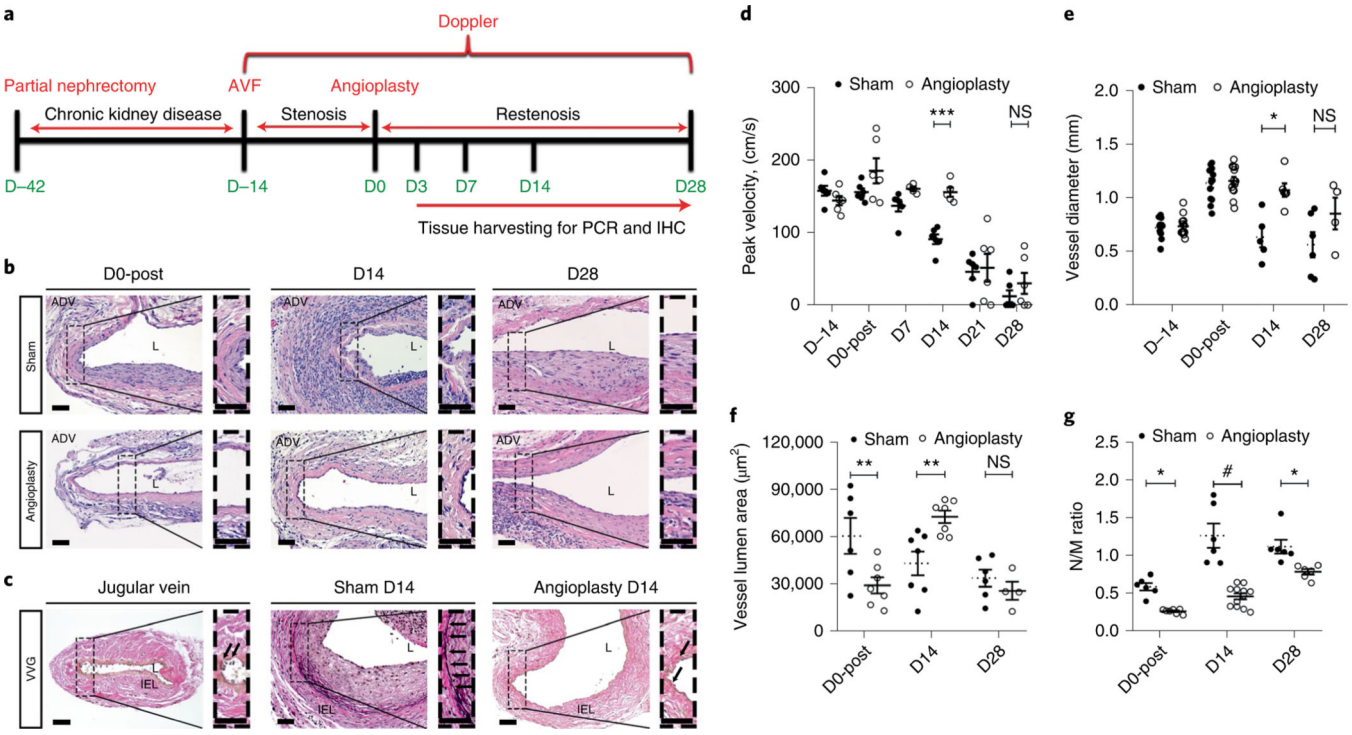

Fig. 2 |. Time course of histomorphometric changes after the angioplasty procedure.

a, Time course of CKD surgery, AVF and angioplasty procedures. **b**, Representative of H&E section of an arterialized EJV after an angioplasty or sham procedure at D0, D14 and D28. At D0, the sham vessel shows obvious arterialization; at D0-post, the vessel shows a reduced neointimal area and cells in the neointimal and media area. At D14, the sham vessel has abundant cellular deposition in the neointimal area, whereas the angioplasty-treated vessel shows less neointima. At D28, no difference can be seen in the neointimal area between the sham- and angioplasty-treated vessels. **c**, Representative Verhoeff–Van Gieson (VVG) staining in a normal contralateral vein, sham and angioplasty-treated vessel at D14. In the normal jugular vein, a single layer of IEL is poorly formed. At D14, in the sham vessels, an obvious IEL is shown between the neointimal area and media area, whereas the angioplasty-treated vessel has an intermittent IEL. **d**, Doppler ultrasound shows that before the angioplasty procedure, peak velocity is similar between sham- and angioplasty-treated vessels. At D14, angioplasty-treated vessels have a significant increase in peak velocity compared to sham vessels. No significant difference is observed at D21 and D28. **e**, At D14, angioplasty-treated vessels have significantly larger vessel diameters than do sham vessels, with no difference at D28. **f**, At D0, angioplasty-treated vessels show a significant decrease in the vessel lumen area compared to sham vessels, but a significant increase at D14 with no difference at D28. **g**, There was a significant decrease in the neointimal area/media area (N/M) ratio in angioplasty-treated vessels compared to sham vessels at D0, D14 and D28. Each time point represents the mean ± s.e.m. of 5–12 animals for each group. Two-way ANOVA with Bonferroni's correction was performed by Graph Pad Prism version 8 (GraphPad Software Inc.). Significant differences are indicated: NS, not significant; $*P < 0.05$; $**P < 0.01$; $***P < 0.001$; $^{\#}P < 0.0001$. Solid arrows indicate IEL. Scale bars: 50 μm.

ADV, adventitia; D, day; L, lumen; D0-post, day 0 post angioplasty; D14, day 14 post angioplasty; D28, day 28 post angioplasty.

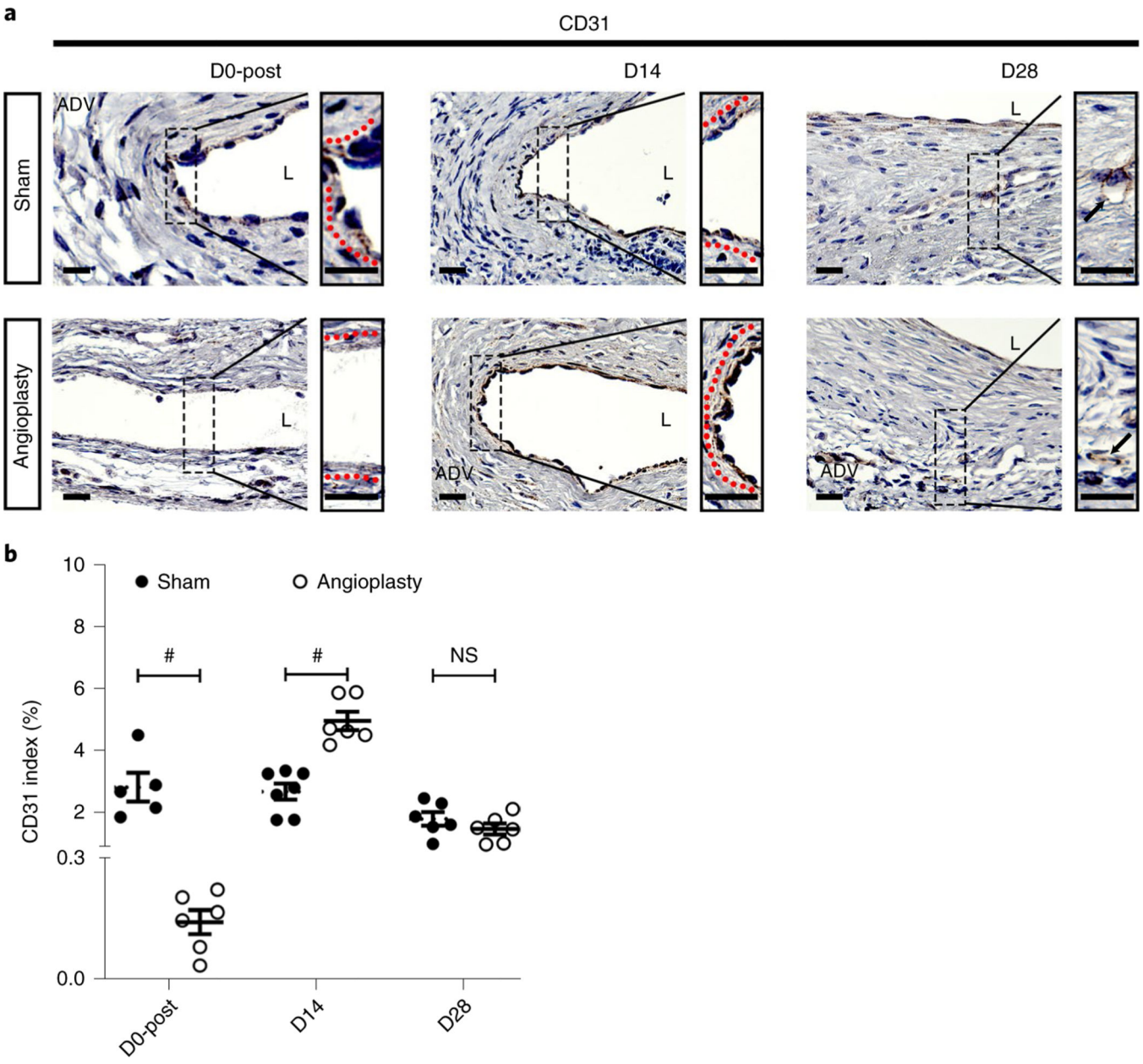

Fig. 3 |. Immunostaining for endothelial cells (CD31$^+$ cells) at different time points.

a, Representative CD31 staining of sham- and angioplasty-treated vessels at D0-post, D14 and D28. At D0, D14 and D28, sham vessels show a discontinuous endothelium layer. There is no endothelial layer in angioplasty-treated vessels at D0-post. At D14, angioplasty-treated vessels have intact endothelium. At D28, CD31$^+$ vessels are present in the neointimal area of both sham- and angioplasty-treated vessels. **b**, Semiquantitative analysis shows a significant decrease in the average CD31 index at D0-post compared to shams, but a significant increase in the index in angioplasty-treated vessels compared to sham controls at D14, with no difference at D28. each time point represents the mean ± s.e.m. of five to seven animals for each group. Two-way ANOVA with Bonferroni's correction was performed by Graph Pad Prism version 8 (GraphPad Software Inc.). Significant differences are indicated: $^{\#}$, $P <$

0.0001. Black solid arrows indicate microvessels, and dashed red lines indicate endothelium layers. Scale bars: 25 μm. ADV, adventitia; L, lumen; NS, not significant.

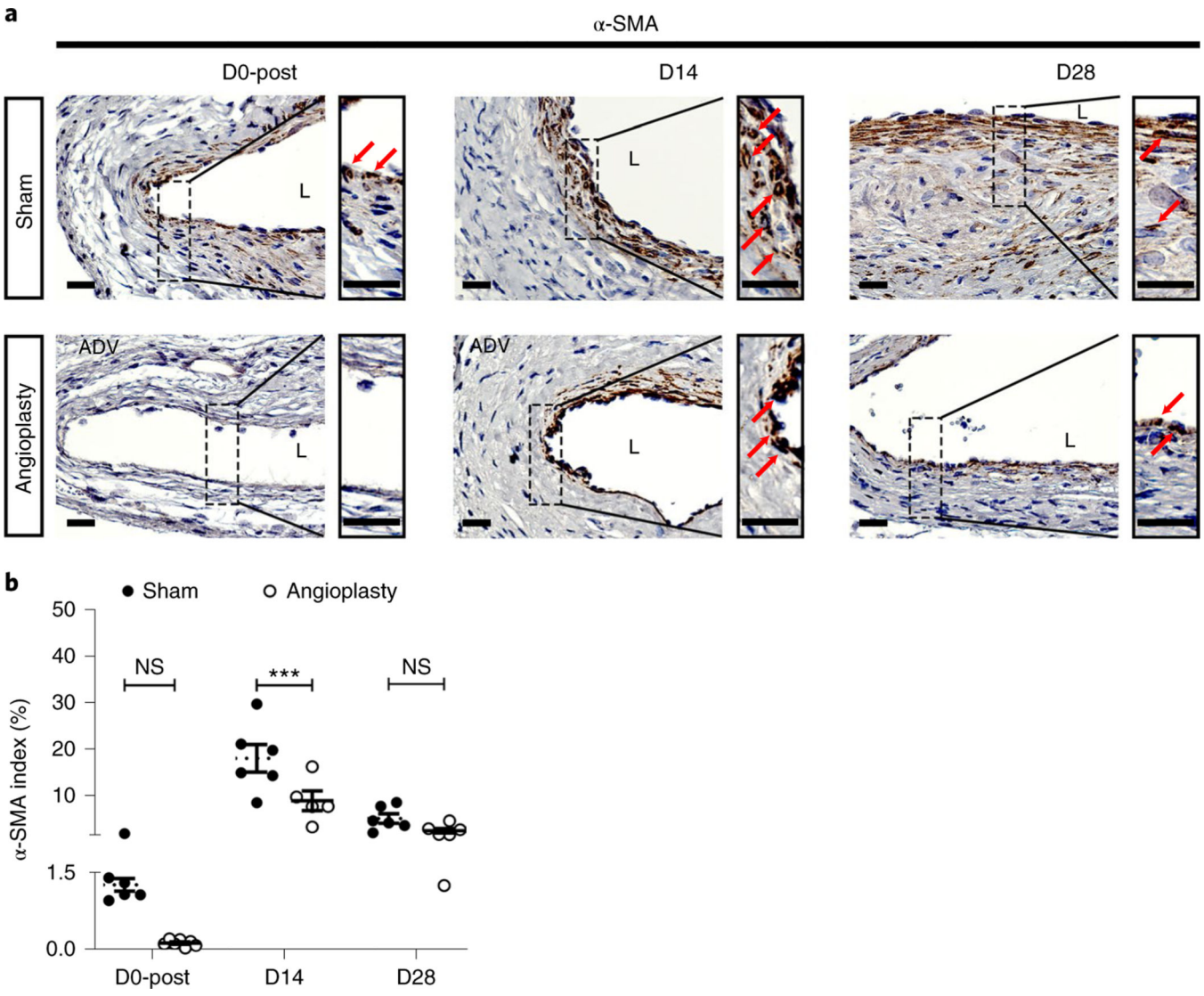

Fig. 4 |. Immunostaining for smooth muscle cells (α-SMA$^+$ cells) at different time points.

a, Representative α-SMA staining of sham- and angioplasty-treated vessels at D0-post, D14 and D28. At D0-post, there are rare α-SMA$^+$ cells in the vessel wall. More α-SMA$^+$ cells can be seen in the sham vessels compared to angioplasty-treated vessels, located in the neointimal and media areas at D14 and D28. b Semiquantitative analysis shows a significant decrease in α-SMA index in angioplasty-treated vessels compared to sham controls at D14, with no difference at D28. Each time point represents the mean ± s.e.m. of five to seven animals for each group. Two-way ANOVA with Bonferroni's correction was performed by Graph Pad Prism version 8 (GraphPad Software Inc.). Significant differences are indicated: ***$P < 0.001$. Red solid arrows indicate positive cells. Scale bars: 25 μm. ADV, adventitia; L, lumen; NS, not significant.

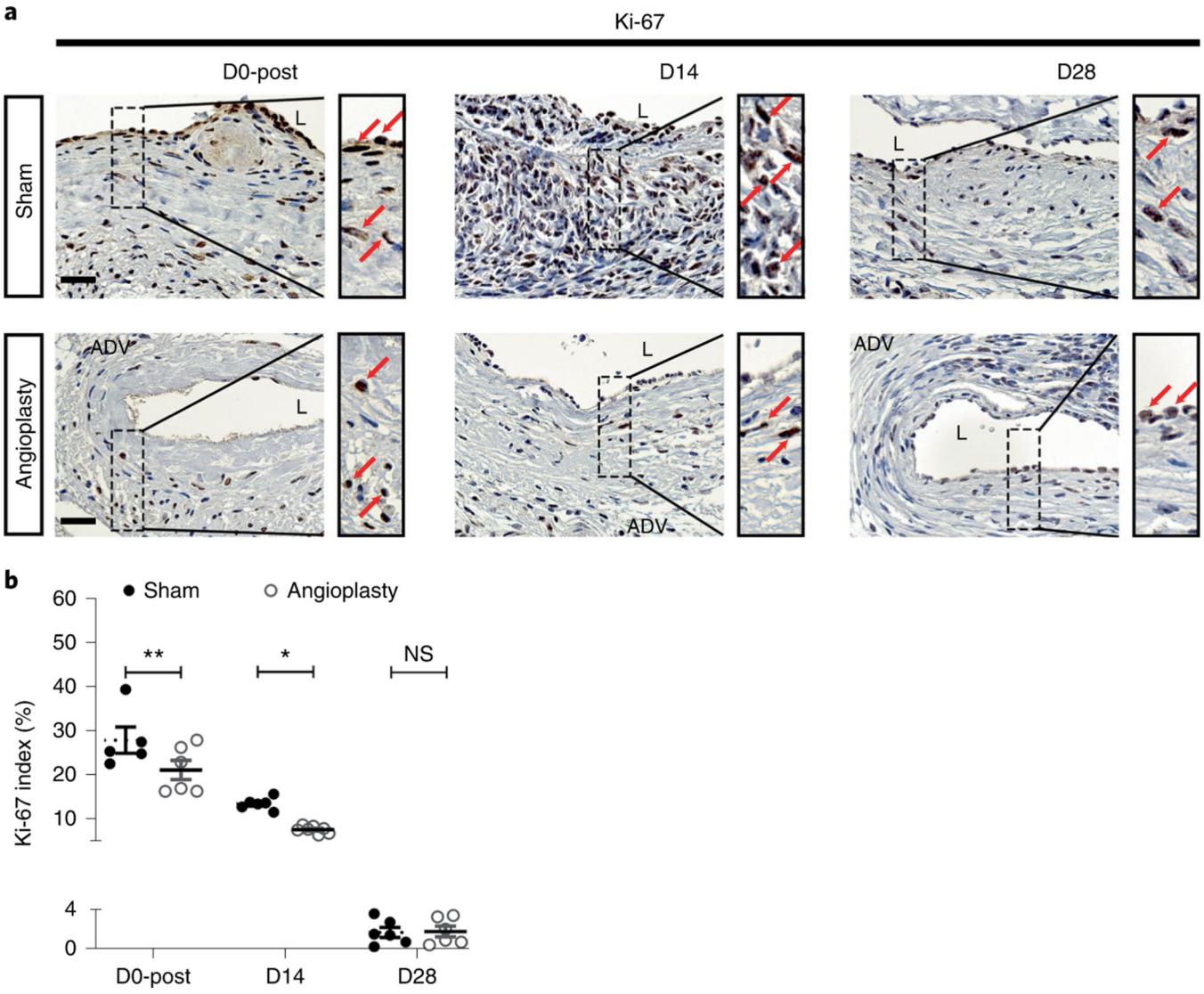

Fig. 5 |. Immunostaining for cellular proliferation (Ki-67) at different time points.

a, Representative Ki-67 staining of sham- and angioplasty-treated vessels at D0-post, D14 and D28. At D0-post, there are more Ki-67$^+$ cells in sham vessels than in angioplasty-treated vessels. At D14, there are abundant Ki-67$^+$ cells in sham vessels, but fewer Ki-67$^+$ cells can be seen in angioplasty-treated vessels. There are no differences between the two groups at D28. **b**, Semiquantitative analysis shows significant decrease in the Ki-67 index in angioplasty-treated vessels compared to sham controls at D0-post and at D14, with no difference at D28. Each time point represents the mean ± s.e.m. of five to seven animals for each group. Two-way ANOVA with Bonferroni's correction was performed by Graph Pad Prism version 8 (GraphPad Software Inc.). Significant differences are indicated: $P < 0.05$; $^{**}P < 0.01$. Red solid arrows indicate positive cells. Scale bars: 25 μm. ADV, adventitia; L, lumen; NS, not significant.

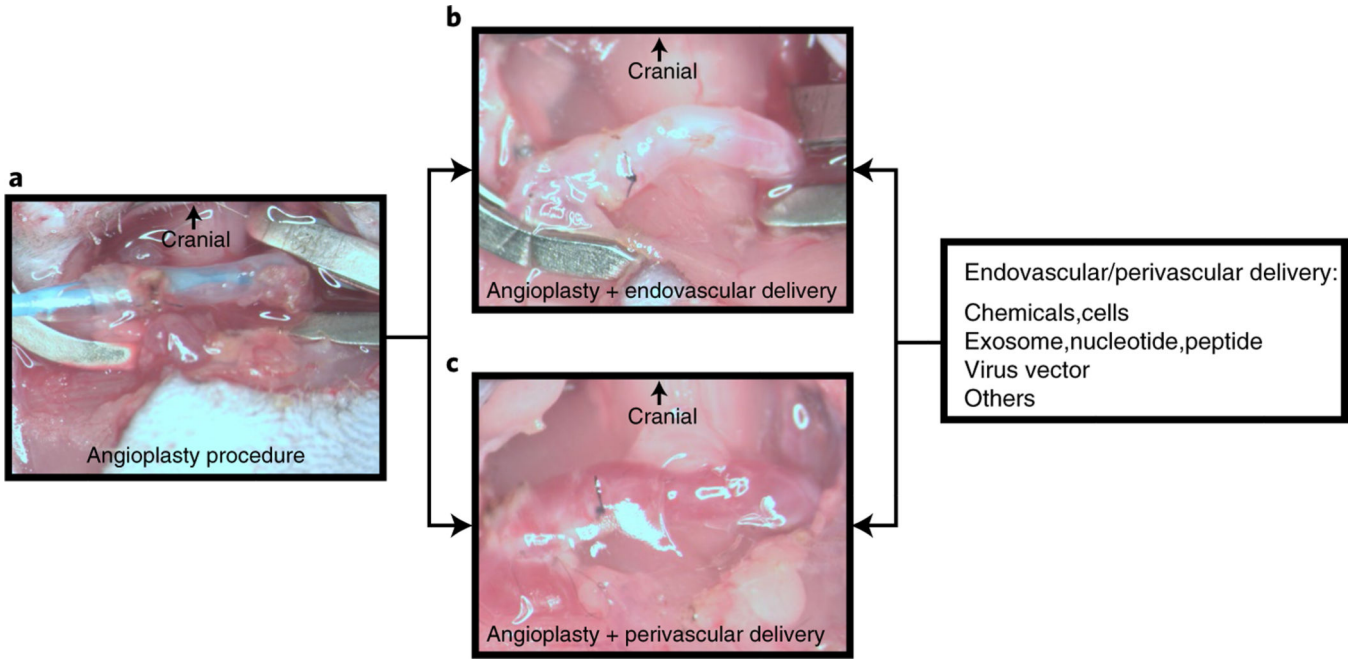

Fig. 6 |. Drug delivery using perivascular and endovascular methods in the murine angioplasty model.

a, Representative image of a successful angioplasty procedure. **b**, After the angioplasty, a drug aimed at preventing restenosis can be allowed to dwell in the lumen with occlusion of the vessel. After 5–30 min, the suture can be loosened after removing the residual drug and flushed with heparinized saline. Finally, the puncture site is closed before the subsequent unclamping process. **c**, After the angioplasty procedure but before incision closure, perivascular drug delivery to the vessel wall can be performed using, for example, biocompatible poly lactic-*co*-glycolic acid nanoparticles loaded with drugs in hydrogel delivered to the outflow vein. Animal procedures in this work were approved by the Mayo Clinic Institutional Animal Care and Use Committee.

Table 1 |

Troubleshooting advice

Step	Problem	Possible reason	Solution
4	Bleeding during dissection of the left common renal arterial bifurcation	Renal vein rupture	Mild bleeding can be treated with gentle compression using a cotton tip
			If excessive bleeding occurs, the animal needs to be excluded from the experiment
	Unable to dissect the renal arterial bifurcation	Renal arterial malformation	Dissect the bifurcation along the left main renal artery. The bifurcation may be close or distal to the renal hilum area
			If there is no renal arterial bifurcation, the animal needs to be excluded from the experiment
5	Lack of ischemia in the left renal upper pole	The ligation is not tight enough	Religate the left renal superior branch artery
14	The REJV is not long enough for AVF creation	Insufficient REJV dissection has been performed	Continue to dissect the REJV until it enters the muscle
			If the distal end is ligated, the animal should be excluded from the experiment
		The REJV has been ligated by mistake	The REJV is larger than the branch vein
15	Bleeding after removing the sternocleidomastoid muscle	There is at least one vessel supplying the sternocleidomastoid muscle	The muscle can be cauterized using an electronic cutter
			Before cutting the muscle, ligate the ends using 6–0 sutures to decrease bleeding
17	Poor patency after creation of the AVF	The anastomosis is too small	Before creating the AVF anastomosis, the ReJV should be gently perfused using heparinized saline
		Heparinization is not adequate	Systemic heparinization of the animal and endovascular flushing with heparinized saline are helpful to prevent thrombosis after AVF creation
18	Bleeding after AVF creation	The stitches are not tight enough	Mild bleeding can be treated with gentle compression using a cotton tip
			Excessive bleeding requires the inflow artery to be clamped. Place an extra suture if needed or exclude the animal from the experiment
29 and 30	The ReJV is not long enough to perform the angioplasty	Insufficient outflow vessel dissection has been performed	Continue to dissect the ReJV and clear the pectoralis major muscle
			Exclude the animal from the experiment
		The puncture point is not at the end of the outflow vessel	The puncture point should be chosen to be as far away as possible from the anastomosis
33	Failure to perform the angioplasty	The balloon catheter cannot be advanced to the anastomosis	The surface of the balloon catheter needs to be soaked in heparinized saline before performing the angioplasty. If there is resistance to advancing the balloon catheter, gentle rotation will be helpful
		The balloon catheter slides out during the angioplasty	During the angioplasty procedure, the balloon catheter should be fixed by microvascular forceps
		The angioplasty-treated vessel ruptures after the angioplasty	The angioplasty needs to be performed at designated pressure using an inflation device
34	Bleeding after angioplasty	The sutures are not tight enough, or a suture is loose	Mild bleeding can be treated with gentle compression using a cotton tip
			Excessive bleeding requires the inflow artery to be clamped. Place an extra suture if needed or exclude the animal from the experiment